Overview: The purpose of this chapter is to introduce the basic features of a *Gaussian-beam wave* in both the plane of the transmitter and the plane of the receiver. Our main concentration of study involves the lowest-order mode or TEM_{00} beam, but we also briefly introduce *Hermite-Gaussian* and *Laguerre-Gaussian beams* as higher-order modes, or additional solutions, of the *paraxial wave equation.* Each of these higher-order modes produces a pattern of multiple spots in the receiver plane as opposed to a single (circular) spot from a lowest-order beam wave. Consequently, the analysis of such beams is more complex than that of the TEM_{00} beam. One advantage in working with the TEM_{00} Gaussian-beam wave model is that it also includes the limiting classical cases of an infinite *plane wave* and a *spherical wave.*

We facilitate the free-space analysis of Gaussian-beam waves by introducing two sets of *nondimensional beam parameters*—one set that characterizes the beam in the plane of the transmitter and another set that does the same in the plane of the receiver. The beam *spot radius* and *phase front radius of curvature*, as well as other beam properties, are readily determined from either set of beam parameters. For example, we use the beam parameters to identify the size and location of the *beam waist* and the *geometric focus.* The consistent use of these beam parameters in all the remaining chapters of the text facilitates the analysis of Gaussian-beam waves propagating through random media.

When optical elements such as aperture stops and lenses exist at various locations along the propagation path, the method of *ABCD ray matrices* can be used to characterize these elements (including the free-space propagation between elements). By cascading the matrices in sequence, the entire optical path between the input and output planes can be represented by a single 2×2 matrix. The use of these ray matrices, which is based on the paraxial approximation, greatly simplifies the treatment of propagation through several such optical elements. In later chapters we will extend this technique to propagation paths that also include atmospheric turbulence along portions of the path.

4.1 Introduction

The mathematical description of a propagating wave involves the notion of a field. Basically, a *field* $u(\mathbf{R}, t)$ is a function of space $\mathbf{R} = (x, y, z)$ and time t that satisfies a partial differential equation. In the case of electromagnetic radiation, the field may be a transverse electromagnetic (TEM) wave, whereas for acoustic waves the field may represent a pressure wave. The governing equation in most cases is the *wave equation*

$$\nabla^2 u = \frac{1}{c^2}\frac{\partial^2 u}{\partial t^2}, \tag{1}$$

where c represents the speed of the propagating wave and ∇^2 is the Laplacian operator defined in rectangular coordinates by

$$\nabla^2 u = \frac{\partial^2 u}{\partial x^2} + \frac{\partial^2 u}{\partial y^2} + \frac{\partial^2 u}{\partial z^2}. \tag{2}$$

For electromagnetic waves, the constant $c = 3 \times 10^8$ m/s is the *speed of light.*

If we assume that time variations in the field are sinusoidal (i.e., a *monochromatic wave*), then we look for solutions of (1) of the form $u(\mathbf{R}, t) = U_0(\mathbf{R})e^{-i\omega t}$, where ω is the *angular frequency* and $U_0(\mathbf{R})$ is the *complex amplitude* of the wave.[1] The substitution of this solution form into Eq. (1) leads to the time-independent *reduced wave equation* (or *Helmholtz equation*)

$$\nabla^2 U_0 + k^2 U_0 = 0, \tag{3}$$

where k is the optical wave number related to the optical wavelength λ by $k = \omega/c = 2\pi/\lambda$.

4.2 Paraxial Wave Equation

For optical wave propagation, we can further reduce the Helmholtz equation (3) to what is called the paraxial wave equation. To begin, let us assume the beam originates in the plane at $z = 0$ and propagates along the positive z-axis. If we also assume the free-space optical field at any point along the propagation path remains rotationally symmetric, then it can be expressed as a function of $r = \sqrt{x^2 + y^2}$ and z. Thus, the reduced wave equation (3) in cylindrical coordinates can be written as

$$\frac{1}{r}\frac{\partial}{\partial r}\left(r\frac{\partial U_0}{\partial r}\right) + \frac{\partial^2 U_0}{\partial z^2} + k^2 U_0 = 0. \tag{4}$$

For reasons of simplification in the solution process, it is customary to first make the substitution $U_0(r, z) = V(r, z)e^{ikz}$ in Eq. (4), which leads to

$$\frac{1}{r}\frac{\partial}{\partial r}\left(r\frac{\partial V}{\partial r}\right) + \frac{\partial^2 V}{\partial z^2} + 2ik\frac{\partial V}{\partial z} = 0. \tag{5}$$

To further simplify Eq. (5), we make use of the so-called "paraxial approximation."

4.2.1 Paraxial approximation

The paraxial approximation is based on the notion that the propagation distance for an optical wave along the z-axis is much greater than the transverse spreading of the wave. Thus, if $\mathbf{R} = (\mathbf{r}, z)$ and $\mathbf{S} = (\mathbf{s}, 0)$ denote two points in space with $\mathbf{r}$ and $\mathbf{s}$

[1] Because the time factor $e^{-i\omega t}$ of the field is usually omitted in wave propagation studies, it is common practice to also refer to the complex amplitude $U_0(\mathbf{R})$ as the (spatial) field.

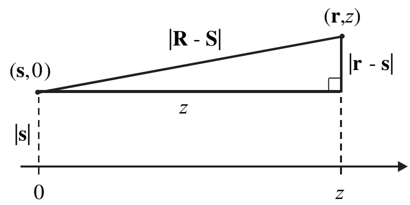

Figure 4.1 Geometry for Eq. (6).

transverse to the propagation axis, then the distance between such points is (see Fig. 4.1)

$$|\mathbf{R}-\mathbf{S}| = \left(z^2 + |\mathbf{r}-\mathbf{s}|^2\right)^{1/2} = z\left(1 + \frac{|\mathbf{r}-\mathbf{s}|^2}{z^2}\right)^{1/2}. \tag{6}$$

If we assume that the transverse distance is much smaller than the longitudinal propagation distance between the points, then we may expand the second factor in (6) in a binomial series to obtain

$$\begin{aligned} |\mathbf{R}-\mathbf{S}| &= z\left(1 + \frac{|\mathbf{r}-\mathbf{s}|^2}{2z^2} + \cdots\right) \\ &= z + \frac{|\mathbf{r}-\mathbf{s}|^2}{2z} + \cdots, \quad |\mathbf{r}-\mathbf{s}| \ll z. \end{aligned} \tag{7}$$

Dropping all remaining terms on the right-hand side of Eq. (7) after the first two shown constitutes what is called the *paraxial approximation.*

As a consequence of the paraxial assumption leading to (7), it follows that

$$\left|\frac{\partial^2 V}{\partial z^2}\right| \ll \left|2k\frac{\partial V}{\partial z}\right|, \quad \left|\frac{\partial^2 V}{\partial z^2}\right| \ll \left|\frac{1}{r}\frac{\partial}{\partial r}\left(r\frac{\partial V}{\partial r}\right)\right|. \tag{8}$$

The inequalities (8) are based on the fact that diffraction effects on the optical wave $V(r, z)$ change slowly with respect to propagation distance z, and also with respect to transverse variations due to the finite size of the beam. The significance of these inequalities is that they permit us to set $\partial^2 V/\partial z^2 = 0$ in Eq. (5), from which we obtain the *paraxial wave equation*[2]

$$\frac{1}{r}\frac{\partial}{\partial r}\left(r\frac{\partial V}{\partial r}\right) + 2ik\frac{\partial V}{\partial z} = 0. \tag{9}$$

There are basically two methods of solution of (9), one called the *direct method* and the other relying on the *Huygens-Fresnel integral* (see Sections 4.3.3 and 4.3.4).

[2]Equation (9) is also known as the *parabolic equation.*

4.3 Optical Wave Models

Most theoretical treatments of optical wave propagation have concentrated on simple field models such as an unbounded plane wave or spherical wave, the latter often taken as a point source. However, in many applications the plane wave and spherical wave approximations are not sufficient to characterize propagation properties of the wave, particularly when focusing and diverging characteristics are important. In such cases the lowest-order Gaussian-beam wave model is usually introduced, limiting forms of which lead to the plane wave and spherical wave models. For certain types of lasers it may also be necessary to introduce the higher-order Gaussian modes in either rectangular or cylindrical coordinates (e.g., see Section 4.7 and also Chap. 17).

4.3.1 Plane wave and spherical wave models

A *plane wave* is defined as one in which the equiphase surfaces (phase fronts) form parallel planes. The mathematical description of a general plane wave in the plane of the transmitter at $z = 0$ is

$$z = 0: \qquad U_0(r, 0) = A_0 e^{i\varphi_0}, \tag{10}$$

where A_0 is a constant that represents the strength or *amplitude* of the wave field and φ_0 is the *phase*. If the plane wave is propagating along the positive z-axis in free space, the complex amplitude at distance z from the transmitter takes the form [1,2]

$$z > 0: \qquad U_0(r, z) = V(r, z)e^{ikz} = A_0 e^{i\varphi_0 + ikz}, \tag{11}$$

where $V(r, z) = A_0 e^{i\varphi_0}$ represents a solution of the paraxial wave equation (9). Hence, the plane wave field remains that of a plane wave with changes occurring only in the phase.

A *spherical wave* is characterized by concentric spheres forming the equiphase surfaces. For a spherical wave emanating from the origin, we have

$$z = 0: \qquad U_0(r, 0) = \lim_{R \to 0} \frac{A_0 e^{ikR}}{4\pi R} \cong A_0 \delta(\mathbf{r}), \tag{12}$$

where $\delta(\mathbf{r})$ is the *Dirac delta function.* At distance z from the transmitter, the solution of the paraxial wave equation for an initial spherical wave leads to [2]

$$z > 0: \quad U_0(r, z) = \frac{A_0}{4\pi z} \exp\left(ikz + \frac{ikr^2}{2z}\right) = A \exp\left[ik\left(z + \frac{r^2}{2z}\right)\right]. \tag{13}$$

Here the amplitude $A = A_0/4\pi z$ is scaled by distance and the phase $\varphi = k(z + r^2/2z)$ has a transverse radial dependency. Because (13) represents the solution of (9) for a point source input (12), it also represents a form of *free-space Green's function* for the paraxial wave equation (see Section 4.3.4).

4.3.2 Lowest-order Gaussian-beam wave

Let us consider the propagation in free space of a lowest-order transverse electromagnetic (TEM) *Gaussian-beam wave*, also called a TEM_{00} wave. It is assumed the transmitting aperture is located in the plane $z = 0$ and the amplitude distribution in this plane is Gaussian with effective beam radius (spot size) W_0 [m], where W_0 denotes the radius at which the field amplitude falls to $1/e$ of that on the beam axis as shown in Fig. 4.2. In addition, the phase front is taken to be parabolic with radius of curvature F_0 [m]. The particular cases $F_0 = \infty, F_0 > 0$, and $F_0 < 0$ correspond to *collimated, convergent*, and *divergent* beam forms, respectively (see Fig. 4.3). If the field of the wave at $z = 0$ has amplitude a_0 $[(W/\mathrm{m}^2)^{1/2}]$ on the optical axis ($r = 0$), it is therefore described by [2]

$$z = 0: \quad U_0(r, 0) = a_0 \exp\left(-\frac{r^2}{W_0^2} - \frac{ikr^2}{2F_0}\right) = a_0 \exp\left(-\frac{1}{2}\alpha_0 k r^2\right), \tag{14}$$

where $r = \sqrt{x^2 + y^2}$ is radial distance from the beam center line and α_0 is a complex parameter related to spot size and phase front radius of curvature according to

$$\alpha_0 = \frac{2}{kW_0^2} + i\frac{1}{F_0}. \quad [\mathrm{m}^{-1}] \tag{15}$$

In comparing the functional form (14) with that of an unbounded plane wave [see Eq. (10)], we identify the *amplitude* and *phase*, respectively, of a Gaussian-beam wave as

$$A_0 = a_0 \exp\left(-\frac{r^2}{W_0^2}\right), \tag{16}$$

$$\varphi_0 = -\frac{kr^2}{2F_0}. \tag{17}$$

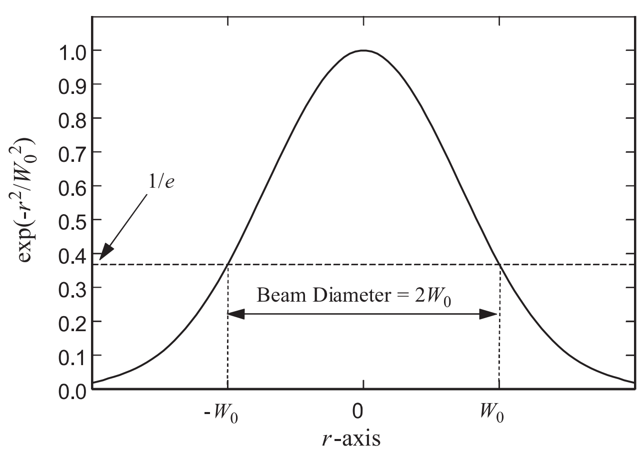

Figure 4.2 Amplitude profile of a Gaussian-beam wave.

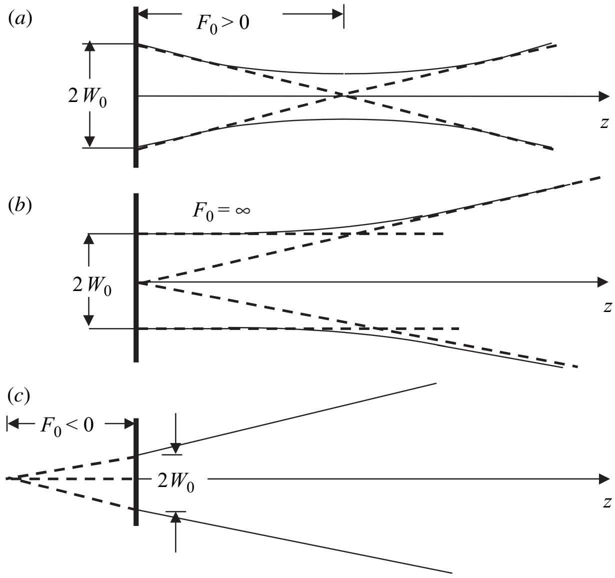

Figure 4.3 (*a*) Convergent beam, (*b*) collimated beam, and (*c*) divergent beam.

Thus, both amplitude and phase of a Gaussian-beam wave depend on the transverse distance r. The negative sign appearing in the phase (17) is a consequence of the sign convention used to define the phase front radius of curvature F_0.

4.3.3 Paraxial equation: direct solution method

To directly solve the paraxial wave equation (9), we will explicitly look for a Gaussian function as a solution. Hence, we start by looking for solutions of the general form [3,4]

$$V(r,z) = A(z)\exp\left[-\frac{1}{p(z)}\left(\frac{\alpha_0 k r^2}{2}\right)\right], \tag{18}$$

where $A(z)$ represents the on-axis complex amplitude of the wave and $p(z)$ is a propagation parameter related to the complex radius of curvature. Clearly, in order that Eq. (18) reduce to the initial Gaussian-beam form given by Eq. (14), these functions must satisfy the *initial conditions*

$$\begin{aligned} p(0) &= 1, \\ A(0) &= a_0 = 1, \end{aligned} \tag{19}$$

where we now set $a_0 = 1$ for mathematical convenience. By substituting Eq. (18) into (9) and simplifying, we obtain

$$\alpha_0^2 k^2 r^2 A(z) + i\alpha_0 k^2 r^2 A(z)p'(z) - 2\alpha_0 k A(z)p(z) + 2ikA'(z)p^2(z) = 0. \tag{20}$$

Next, by setting terms involving like powers of r to zero, we obtain the pair of simple first-order differential equations

$$r^2: \quad p'(z) = i\alpha_0 = -\frac{1}{F_0} + i\frac{2}{kW_0^2}, \tag{21}$$

$$r^0: \quad A'(z) = -\frac{i\alpha_0}{p(z)}A(z) = -\frac{p'(z)}{p(z)}A(z). \tag{22}$$

The simultaneous solution of Eqs. (21) and (22) together with the initial conditions (19) yield

$$\begin{aligned} p(z) &= 1 + i\alpha_0 z = 1 - \frac{z}{F_0} + i\frac{2z}{kW_0^2}, \\ A(z) &= \frac{1}{p(z)} = \frac{1}{1 + i\alpha_0 z}. \end{aligned} \tag{23}$$

In summary, the complex amplitude at distance z from the source is the Gaussian-beam wave

$$\begin{aligned} U_0(r, z) = V(r, z)e^{ikz} &= \frac{1}{1 + i\alpha_0 z}\exp\left[ikz - \frac{1}{2}\left(\frac{\alpha_0 k}{1 + i\alpha_0 z}\right)r^2\right] \\ &= \frac{1}{1 + i\alpha_0 z}\exp\left[ikz + \frac{ik}{2z}\left(\frac{i\alpha_0 z}{1 + i\alpha_0 z}\right)r^2\right], \end{aligned} \tag{24}$$

where the final form of (24) is chosen for later mathematical convenience.

4.3.4 Paraxial equation: Huygens-Fresnel integral

The Huygens-Fresnel integral provides another method of analysis that leads to the same result as Eq. (24) for the complex amplitude at position z along the propagation path, but has the distinct advantage that it can be extended to the case where the propagation path includes several optical elements arbitrarily distributed along the path (e.g., see Sections 4.9 and 4.10). In the present formulation, the complex amplitude at propagation distance z from the source is represented by the *Huygens-Fresnel integral* [4,5]

$$U_0(\mathbf{r}, z) = -2ik\int\!\!\int_{-\infty}^{\infty} G(\mathbf{s}, \mathbf{r}; z)U_0(\mathbf{s}, 0)d^2s, \tag{25}$$

where $U_0(\mathbf{s}, 0)$ is the optical wave at the source plane and $G(\mathbf{s}, \mathbf{r}; z)$ is the *free-space Green's function.* In general, the free-space Green's function is a spherical wave which, under the paraxial approximation, can be expressed as [recall Eqs. (7) and (13)]

$$G(\mathbf{s}, \mathbf{r}; z) = \frac{e^{ik|\mathbf{R}-\mathbf{S}|}}{4\pi|\mathbf{R} - \mathbf{S}|} \cong \frac{1}{4\pi z}\exp\left[ikz + \frac{ik}{2z}|\mathbf{s} - \mathbf{r}|^2\right]. \tag{26}$$

Although we will not do so here (see Example 4 in Worked Examples), it can be shown that Eq. (25) represents a formal solution of the initial value problem

$$\begin{aligned} &\frac{1}{r}\frac{\partial}{\partial r}\left(r\frac{\partial V}{\partial r}\right)+2ik\frac{\partial V}{\partial z}=0,\\ &V(r,0)\equiv U_0(r,0)=\exp\left(-\frac{r^2}{W_0^2}-\frac{ikr^2}{2F_0}\right), \end{aligned} \tag{27}$$

where $V(r,z)=U_0(r,z)e^{-ikz}$. Instead, we illustrate that the optical wave represented by Eq. (25) is the same as that given by Eq. (24). We start by writing the complex amplitude of the Gaussian-beam wave at the source plane $z=0$ as

$$U_0(\mathbf{s},0)=\exp\left(-\frac{1}{2}\alpha_0 ks^2\right)=\exp\left[\frac{ik}{2z}(i\alpha_0 z)s^2\right]. \tag{28}$$

The substitution of Eq. (28) into Eq. (25) yields

$$\begin{aligned} U_0(\mathbf{r},z)&=-\frac{ik}{2\pi z}\exp\left(ikz+\frac{ik}{2z}r^2\right)\iint_{-\infty}^{\infty}\exp\left(-\frac{ik}{z}\mathbf{r}\cdot\mathbf{s}\right)\exp\left[\frac{ik}{2z}(1+i\alpha_0 z)s^2\right]d^2s\\ &=-\frac{ik}{2\pi z}\exp\left(ikz+\frac{ik}{2z}r^2\right)\int_0^{\infty}\int_0^{2\pi}\exp\left(-\frac{ik}{z}rs\cos\theta\right)\\ &\quad\times\exp\left[\frac{ik}{2z}(1+i\alpha_0 z)s^2\right]s\,d\theta\,ds, \end{aligned} \tag{29}$$

where we have changed to polar coordinates in the second step, i.e., $d^2s=s\,d\theta\,ds$. Performing the inside integration yields (integral #9 in Appendix II)

$$\int_0^{2\pi}\exp\left(-\frac{ik}{z}rs\cos\theta\right)d\theta=2\pi J_0\left(\frac{krs}{z}\right), \tag{30}$$

where $J_0(x)$ is a Bessel function of the first kind and order zero [6]. The remaining integration on s gives us (integral #10 in Appendix II)

$$\begin{aligned} U_0(r,z)&=-\frac{ik}{z}\exp\left(ikz+\frac{ik}{2z}r^2\right)\int_0^{\infty}sJ_0\left(\frac{krs}{z}\right)\exp\left[\frac{ik}{2z}(1+i\alpha_0 z)s^2\right]ds\\ &=\frac{1}{1+i\alpha_0 z}\exp\left[ikz+\frac{ik}{2z}\left(\frac{i\alpha_0 z}{1+i\alpha_0 z}\right)r^2\right], \end{aligned} \tag{31}$$

which is the same as Eq. (24). Thus, we have established the equivalence of the direct method and the Huygens-Fresnel integral.

4.4 Diffractive Properties of Gaussian-Beam Waves

Early studies of the diffractive characteristics of Gaussian-beam waves for the design and analysis of laser systems include those of Refs. [3,7–12]. Kogelnik and Li [3] provide a good review of the basic theory of laser beams and resonators, and they also discuss the use of *ABCD* ray matrices to illustrate Gaussian-beam wave propagation through optical structures. Graphical representations of Gaussian-beam wave propagation in optical resonators with circle diagrams were first proposed by Collins [8], and Li [9] extended the notion to the case of dual circles. Arnaud [13] suggested a graphic method for determining the beam parameters that is essentially the $y\bar{y}$ diagram method introduced by Delano [7]. Kessler and Schack [14] illustrated the utility of the $y\bar{y}$ diagram method as a helpful design tool for synthesizing and analyzing optical systems. Andrews et al. [15] developed a method of Gaussian-beam wave analysis through the use of two pairs of Gaussian-beam parameters that are linked through an elementary conformal transformation. The basic beam characteristics are readily identified in either plane through simple geometric and analytic relations. In this chapter we review the basic notation and relations introduced in Ref. [15], which in turn are utilized in our subsequent analysis of Gaussian-beam wave propagation through random media. We believe the consistent use of these beam parameters throughout the text can assist the development of physical intuition for the reader.

4.4.1 Input plane beam parameters

Let us consider the line-of-sight propagation of a Gaussian beam from the input plane positioned at $z = 0$ to the output plane at $z > 0$. By *line of sight*, we mean the transmitter and receiver are able to "see" each other (no optical elements exist between input and output planes). To begin, we express the propagation parameter $p(z)$ in the form [see Eqs. (23)]

$$p(z) = 1 + i\alpha_0 z = \Theta_0 + i\Lambda_0, \tag{32}$$

where Θ_0 and Λ_0 are the real and imaginary parts of $p(z)$ defined by

$$\Theta_0 = 1 - \frac{z}{F_0}, \quad \Lambda_0 = \frac{2z}{kW_0^2}. \tag{33}$$

Next, by making the observation

$$\begin{aligned}\frac{i\alpha_0 z}{1 + i\alpha_0 z} &= 1 - \frac{1}{\Theta_0 + i\Lambda_0}\\ &= \frac{\Theta_0(\Theta_0 - 1) + \Lambda_0^2}{\Theta_0^2 + \Lambda_0^2} + i\frac{\Lambda_0}{\Theta_0^2 + \Lambda_0^2}\end{aligned}$$

and writing

$$p(z) = \sqrt{\Theta_0^2 + \Lambda_0^2}\exp\left(i\tan^{-1}\frac{\Lambda_0}{\Theta_0}\right), \tag{34}$$

it follows from Eq. (24) that

$$\begin{aligned} U_0(r,z) &= \frac{1}{1+i\alpha_0 z}\exp\left[ikz + \frac{ik}{2z}\left(\frac{i\alpha_0 z}{1+i\alpha_0 z}\right)r^2\right] \\ &= \frac{1}{\sqrt{\Theta_0^2+\Lambda_0^2}}\exp\left(-\frac{r^2}{W^2}\right)\exp\left[i\left(kz-\varphi-\frac{kr^2}{2F}\right)\right], \end{aligned} \tag{35}$$

where φ, W, and F represent the *longitudinal phase shift, spot size radius*, and *radius of curvature* at position z along the propagation path. These quantities are defined, respectively, in terms of beam parameters Θ_0 and Λ_0 by

$$\varphi = \tan^{-1}\frac{\Lambda_0}{\Theta_0}, \tag{36}$$

$$W = W_0\sqrt{\Theta_0^2+\Lambda_0^2}, \tag{37}$$

$$F = \frac{kW_0^2}{2}\left[\frac{\Lambda_0\left(\Theta_0^2+\Lambda_0^2\right)}{\Theta_0(1-\Theta_0)-\Lambda_0^2}\right] = \frac{F_0\left(\Theta_0^2+\Lambda_0^2\right)(\Theta_0-1)}{\Theta_0^2+\Lambda_0^2-\Theta_0}. \tag{38}$$

Because they involve beam characteristics at the input plane (transmitter), we refer to the pair of nondimensional quantities Θ_0 and Λ_0 as *input plane* (or *transmitter*) *beam parameters.* The parameter Θ_0 is also called the *curvature parameter* and Λ_0 is the *Fresnel ratio* at the input plane. For fixed path length $z = L$ and radius of curvature F_0, the curvature parameter identifies collimated, convergent, and divergent beam forms, respectively, according to $\Theta_0 = 1$, $\Theta_0 < 1$, and $\Theta_0 > 1$.

By examination of Eq. (35), we recognize that the input plane beam parameters Θ_0 and Λ_0 characterize the refractive (focusing) and diffractive changes, respectively, in the on-axis amplitude of the Gaussian beam. In particular, after propagating a distance z, the on-axis amplitude of the beam takes the form

$$A = \frac{1}{\sqrt{\underbrace{(1-z/F_0)^2}_{\textbf{refraction}}+\underbrace{(2z/kW_0^2)^2}_{\textbf{diffraction}}}} = \frac{1}{\sqrt{\Theta_0^2+\Lambda_0^2}}. \tag{39}$$

For a Gaussian-beam wave, the longitudinal phase shift (36) varies from zero at the transmitter up to π as the propagation path length becomes infinite (see Section 4.5). In the limiting case of a plane wave, however, this phase shift is always zero because $\Lambda_0 = 0$. Except for a convergent beam, diffraction effects cause the spot size radius of the beam (37) to increase steadily along the entire propagation path. That is, the spot radius will initially decrease for a transmitted convergent beam until it reaches the waist region and then increase in accordance with the spot radius of a collimated beam [see Fig. 4.3(a)]. To illustrate the general behavior of the phase front radius of curvature (38) along the propagation path, we plot the ratio F/F_0 as a function of scaled distance z/F_0 in Fig. 4.4 for a convergent beam in which $2F_0/kW_0^2 = 1$. Observe that the radius of curvature has a positive

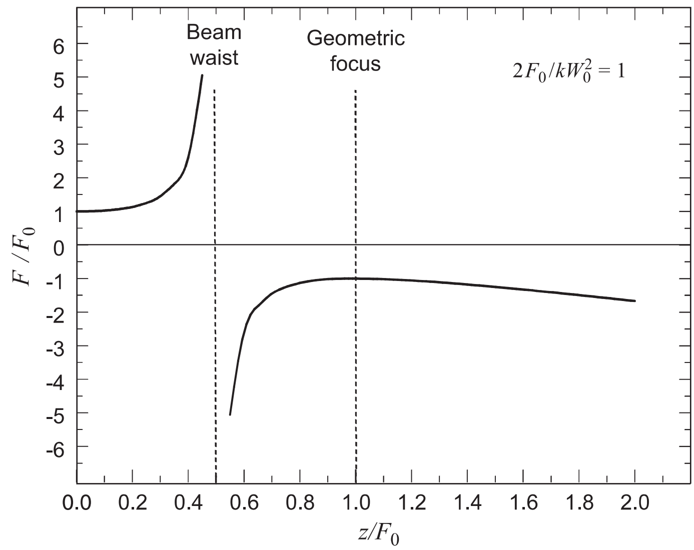

Figure 4.4 Scaled phase front radius of curvature as a function of scaled propagation distance.

sign prior to the beam waist (the minimum beam spot size) and becomes unbounded at the waist (i.e., the phase front is planar). Upon passing through the waist region, the phase front radius of curvature changes sign to negative and remains so for the rest of the path. Also, at the geometric focus the phase front radius of curvature is always the negative of that at the transmitter.

The *irradiance* or *intensity* of the optical wave is the squared magnitude of the field. Thus, at the receiver the irradiance is

$$\begin{aligned} I^0(r,z) &= |U_0(r,z)|^2 \\ &= I^0(0,z)\exp\left(-\frac{2r^2}{W^2}\right), \qquad [\mathrm{W/m^2}] \end{aligned} \tag{40}$$

where

$$I^0(0,z) = \frac{W_0^2}{W^2} = \frac{1}{\Theta_0^2 + \Lambda_0^2} \tag{41}$$

is the *on-axis irradiance.* Finally, because we assume no loss of power, the total power at the receiver (or transmitter) is

$$P = \iint_{-\infty}^{\infty} I^0(r,0)d^2r = \iint_{-\infty}^{\infty} I^0(r,z)d^2r = \frac{1}{2}\pi W_0^2. \quad [\mathrm{W}] \tag{42}$$

4.4.2 Output plane beam parameters

Although the beam characteristics (36)–(38) are well defined using the input plane beam parameters, it is instructive to present a parallel development of these